Conformational Free Energy of Lattice Polyelectrolytes with Fixed End Points. 2. The Swelling Behavior of a Permanent Network of Lattice Polyelectrolytes

Th. M. A. O. M. Barenbrug,*,† D. Bedeaux, and J. A. M. Smit

Leiden Institute of Chemistry, Gorlaeus Laboratories, Leiden University, P.O. Box 9502, 2300 RA Leiden, The Netherlands

Received March 6, 1998; Revised Manuscript Received September 28, 1998

ABSTRACT: "Lattice polyelectrolytes" are conceived as self-avoiding walks on a cubic lattice, bearing monovalent, equidistantly fixed, discrete charges, located at vertexes of the lattice, along the followed path. The electrostatic interactions between these charges are described by a Debye−Hückel potential. Recently (part 1: Barenbrug, Th. M. A. O. M.; Smit, J. A. M.; Bedeaux, D. *Macromolecules* **1997**, *30*, 605) we obtained the conformational free energy of a single lattice polyelectrolyte with fixed end points, using Monte Carlo calculations. Here (part 2) we exploit this result to develop a model in which the charged lattice chains are incorporated in a network with tetrafunctional cross-links. This network may serve as a model for polyelectrolyte gels, in particular with respect to their swelling properties as a function of charge and salt content. The salt-depending swelling of a real gel is semiquantitatively predicted.

1. Introduction

The swelling behavior of polyelectrolyte gels in solutions containing salt ions is important from a theoretical as well as a practical viewpoint.[1] Usually these gels are visualized as permanent, three-dimensional polymer networks bearing negative charges. Well-known examples are PSSA (polystyrene sulfonic acid) gels and P(M)AA (poly(meth)acrylic acid) gels, respectively possessing strong and weak acid groups. In addition they contain small amounts of cross-link agent, needed to form the stable network structure. Obviously the experimentally prepared gels show many defects, like heterodispersity of the chain lengths, loops, loose ends, entanglements, or even interpenetrating networks. These defects cannot easily be taken into account in theoretical models. Generally, however, these imperfections are believed to disturb only the local properties and not to change the global behavior of the gel.

One of the most striking features of polyelectrolyte gels is their ability to absorb large amounts of water and to swell strongly during this process. This swelling can be attenuated by adding salt to the external water phase. The physical picture underlying this phenomenon is nowadays rather well understood. A gel immersed in pure water will swell till its free energy has reached a minimum value with respect to the swelling volume. The derivative of the free energy with respect to the volume is just the negative osmotic pressure, which is therefore equal to zero. Hence, at equilibrium the different contributions to this osmotic pressure counterbalance each other. Some of them, e.g., the contributions from the counterions, from the charge repulsions, and from the solvent−polymer mixing interactions, induce swelling of the gel, whereas deswelling of the gel is driven by the network elasticity. When a swollen gel is immersed in a salt solution, deswelling is observed, which sometimes looks like a collapse. By adding salt, the Donnan osmotic pressure difference, exerted by the small ions, is decreased. Also the charges fixed on the polymer matrix are better screened. The salt effect, however, is rather subtle, as it gives rise to many cooperative effects. Recently we developed a gel model for semiflexible polyelectrolyte chains in which the osmotic pressure balance was considered in detail.[2]

In the past decades many theories have been formulated that use the picture for swelling sketched above. Globally these theories fall into two categories. The more recent scaling theories[3−5] employ the blob picture, which requires sufficiently long, flexible, weakly charged chains. In these theories not only the dilute but also the semidilute regime are introduced, so interchain interactions are incorporated**,** which makes these models suitable for shrunken gels but less appropriate to describe stiff chains, the length of which is of the same order as their persistence length. The other category deals with theories that provide more explicit descriptions of the osmotic pressures, rather than in terms of scaling laws. Many attempts[6−9] simply combine the network pressure with the osmotic pressure of the counterions. Katchalsky[10−12] was the first to consider the free energy of network charge interactions. His theory and many subsequent theories are mainly based on single chain properties, as only intrachain interactions are considered. However, due to the neglect of the effects of charge interactions on the Gaussian chain statistics, all these theories overestimate the charge dependence of the degree of swelling, particularly in the case of highly charged gels.[13−17] Therefore they are best applicable to weakly charged, (but still) strongly swollen gels.

In this paper we conceive a simple model gel of lattice polyelectrolytes to study its swelling behavior. It is based on the single chain approach, but the charge repulsion is better estimated by extending Katchalsky's original expression, and by using our recent Monte Carlo results (part 1[13]). Moreover, the uncharged lattice chains are taken either as random walks (RWs) or as

†Delft University of Technology, Laboratory for Aero- and Hydrodynamics, Rotterdamseweg 145, 2628 AL Delft, The Netherlands.

* To whom correspondence should be addressed.

10.1021/ma980355r CCC: $18.00
Published on Web 12/18/1998

self-avoiding walks (SAWs). In section 2 we specify the model and we outline the basics of the swelling theory, following our previous work.[2] Subsequently we derive the different contributions to the osmotic pressure: (1) the network pressure involving the tensile force exerted by the uncharged chains (Π_{bare}), combined with the electrostatic term (Π_{rep}), (2) the Donnan osmotic pressure (Π_{Donnan}), and (3) the Flory−Huggins mixing term (Π_{mix}). From the balance of these pressures at swelling equilibrium we solve the relevant swelling variables. In section 3, the latter are discussed as a function of the external salt concentration and of the linear charge density of the chains and as such compared with recent experimental findings. In section 4 the main conclusions are summarized.

2. Theory of Swelling of Polyelectrolyte Gels

2.1. General. As discussed in most treatments on this subject,[2−4,9−12,14−18] the swelling behavior of a polyelectrolyte gel, immersed in a salt solution, is essentially governed by four contributions to the total osmotic pressure Π, which equals zero in equilibrium,

$$\Pi = \Pi_{bare} + \Pi_{rep} + \Delta\Pi_{Donnan} + \Pi_{mix} \quad (2.1.1)$$

Π_{bare} is the contribution of the bare (uncharged) polymer chains. Π_{rep} is the pressure contribution caused by the interacting charges on the polyelectrolyte chains, so that $\Pi_{bare} + \Pi_{rep} = \Pi_{network}$, the total contribution of the network to the osmotic pressure of the gel. $\Delta\Pi_{Donnan}$ is the contribution due to the difference in concentrations of the small ions in the internal and external solution, caused by Donnan exclusion of external salt by the counterions. Π_{mix} is the contribution from the mixing of polymer segments and solvent.

In equilibrium the total free energy of the gel is at a minimum with respect to its swelling volume, so that $\Pi = -(\partial F/\partial V)_T = 0$.

In previous work[2] we studied the different contributions to the osmotic pressure in detail for a model gel consisting of semiflexible chains, arranged in a simple cubic manner, implying hexafunctional cross-links.

The gel model described here consists of flexible lattice polyelectrolytes, all of the same length and connected by tetrafunctional cross-links (see Figure 1). Furthermore, a remaining and important simplification of the model is the neglect of the interchain interactions, including the electrostatic ones. For our model chains, like before,[13,18] we set the bond length a to 2.515 Å, to mimic chains of poly(acrylic acid) (PAA). This choice of the bond length sets the length of the bare persistence length of the chain to a value of[18] $1.42a$. This is much smaller than its experimental value of about 10 Å. We return to this point in section 3.4.

In this section we discuss briefly the differences between the previous[2] and present approach. Clearly, the differences concern primarily the chain behavior and the different geometry of the gel structure. In this paper the chains have the flexible properties of lattice polyelectrolytes, instead of being semiflexible. As in our previous approach, we have split the pressure exerted by the network in (a) the elastic contribution from the bare (=uncharged) chains and (b) the contribution from the charges that reside on the chain and repel each other (see eq 2.1.1). The pressure contribution from the bare chains is studied more thoroughly in this paper;

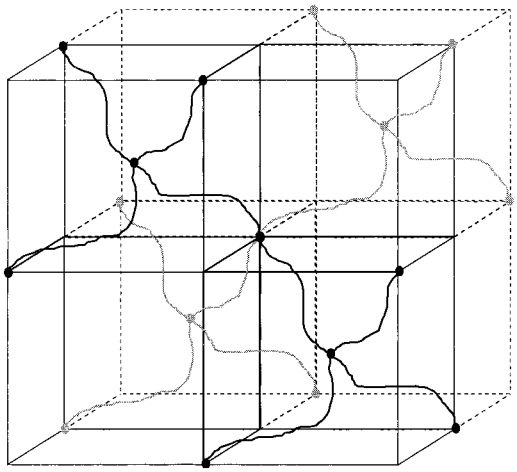

Figure 1. Sketch of the unit cube of an "ideal" network of "lattice polyelectrolytes" linked by tetrafunctional cross-links. The unit cube consists of eight subcubes. Four of these contain polyelectrolyte chains, ordered in a tetrahedral fashion. The polyelectrolyte molecules in the foreground subcubes are solid, in the background shaded. The other four subcubes have four cross-links on their vertexes but do not contain polyelectrolyte molecules.

for the electrostatic contribution we take the expressions derived in part 1.[13]

Furthermore, the different arrangement of the polyions in the model gel, using tetrafunctional instead of hexafunctional cross-links, implies that small adaptations must be made in the expressions for the other pressure terms. As these modifications can be made in a very straightforward way, we will not discuss them in very much detail.

We use the same notation as in part 1:[13] R is the end-to-end distance of the lattice chain, which consists of n steps or bonds. In counting the number of lattice (or mass) points, which we call segments, we include the ends of the chain. Thus the number of segments is $n + 1$; the bond length a has been defined before; L is the contour length of the chain (so $L = na$); q is the number of charges, which reside on the segments, so that $q \in \{0, 1, .., n + 1\}$; κ is the reciprocal Debye length; N_A is Avogadro's number; Q is the Bjerrum length ($Q \equiv e^2/4\pi\epsilon kT$), where e is the charge of an electron, ϵ is the permittivity of the medium, k is Boltzmann's constant, and T is the absolute temperature. All quantities are expressed in SI units. Furthermore we define the relative extension of the chains by $x = R/L$. Free energies are represented by a capital F (F/kT in dimensionless, "reduced" form); tensile forces are represented by a small f (fL/kT, respectively). Contributions from the bare chain have subscript 0; contributions due to network charge interactions have subscript q. The total tensile force exerted by the network chains is considered to be additive,

$$f = f_0 + f_q \quad (2.1.2)$$

As discussed previously,[2] the different contributions to the gel osmotic pressure depend on the value of x, the relative extension of the chains, which governs (a) $\Pi_{network}$, (b) the concentration of chains in the gel (and thus Π_{mix}), and therefore (c) the concentration of the counterions of the polymer, which, together with the external salt concentration, determines the internal salt concentration (and thus $\Delta\Pi_{Donnan}$). The x value for which the total osmotic pressure is zero is the equilibrium

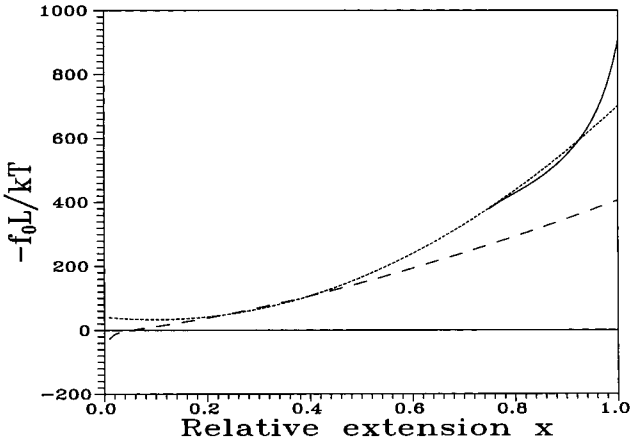

Figure 2. Plot of the negative of the reduced bare tensile force, f_0L/kT, of a SAW chain of 160 segments, versus its relative extension x (=R/L). Shown are the *derivative* of the 3rd (dots) and 10th (solid curve) degree polynomial fit to the simulation data for the reduced free energy (F_0/kT) of the bare chain with fixed endpoints. The dashed curve is the theoretical curve for the reduced tensile force exerted by a SAW, as proposed by Des Cloizeaux (see eqs 2.2.3 and 2.2.5).

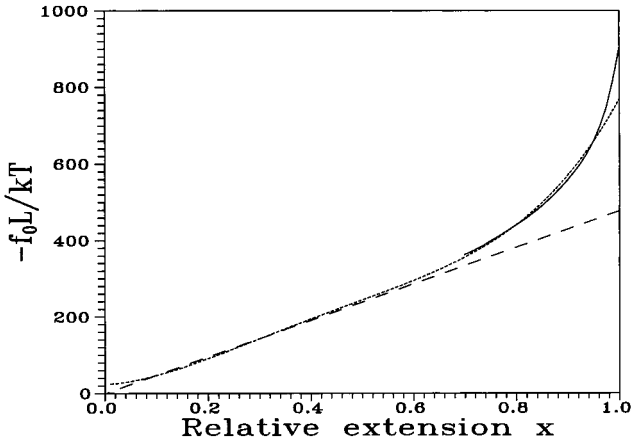

Figure 3. Plot comparable to Figure 2, but now for a RW chain of 160 segments. The dotted curve is the derivative of the best fit curve of the fifth degree to the simulation data (for $0.1 < x < 0.9$). The solid curve is derived from the 10th degree fit polynomial to the simulation data for high x-values. The dashed curve is the reduced tensile force exerted by a corresponding Gaussian chain (eq 2.2.4).

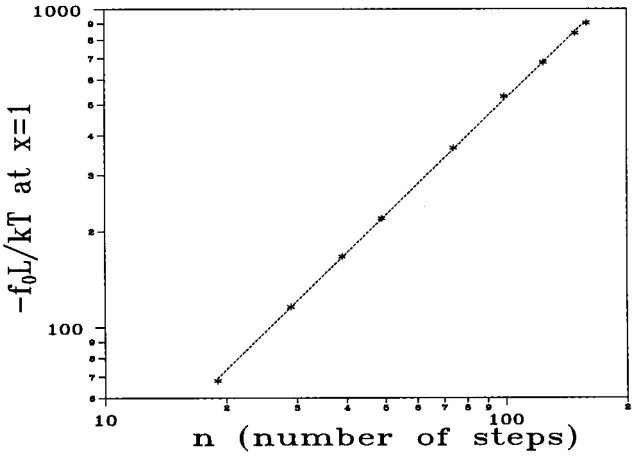

Figure 4. Negative of the reduced bare tensile force f_0L/kT at complete extension ($x = 1$) for RWs as well as for SAWs (results are identical) versus their number of steps, n.

extension, which determines the equilibrium degree of swelling (cf. eq 2.1.1). The volume of the gel is denoted V. V_0 is the *dry* volume of the gel. It is calculated by multiplying the molar volume per segment, V_m, by the number of segments (in mol) present in the unit cube. For V_m, we take 45.4×10^{-6} m^3, to mimic PAA. V_{min} is the volume the gel occupies in excess salt and may be regarded the swelling volume of the uncharged gel. In this case the gel still contains some liquid, so that generally $V_{min} > V_0$. V_{max} is the volume the gel would have at complete extension of the chains.

2.2. Tensile Force of a Bare Chain in the Network. To obtain an expression for the tensile force f_0 exerted by the bare chain (see eq 2.1.2), we first fitted the data for the free energy F_0 of the uncharged lattice chains with fixed endpoints to polynomials of different degrees in the relative extension x. Then differentiating the fit curve for $F_0(x)/kT$ with respect to x and taking the negative, one obtains the expression for the reduced tensile force, f_0L/kT. Note that due to this definition the tensile force is negative (contractive). This force was obtained for both the simulation data for self-avoiding walks (SAWs), which simulate polymer chains in a good solvent, and for the exact results for ordinary random walks (RWs, see Appendix 1 of part 1[13]). RWs simulate, to a fair approximation, polymer chains in a θ-solvent.

The data for the reduced free energy (F_0/kT) of bare lattice chains with fixed endpoints can be represented by polynomials in the relative extension x. For the SAW data (see part 1[13]) a third degree polynomial gives satisfactory results for $0.2 \le x \le 0.9$. For $19 \le n \le 159$ the fit coefficients are linearly dependent on n (see the Appendix). We use this dependency for interpolation and extrapolation to other values of n. For RWs, and in the same range of x values, we use a fifth degree polynomial, using the exact endpoint distribution of a RW on a cubic lattice calculated in Appendix 1 of part 1.[13] In the swollen gel smaller extensions ($x \le 0.2$) are not relevant. For very high extensions the free energy increases steeply with x and must be described by a higher (we used a 10th) degree polynomial.

In Figure 2 we plotted the results for the reduced bare tensile force f_0L/kT exerted by an uncharged SAW chain of 160 segments, versus its relative extension. Shown are the derivative of the general third degree curve for F_0/kT over the entire x range and of the 10th degree curve, valid for the range of large values of x. In the intermediate range of x values ($0.2 \le x \le 0.9$) the derivative of the 10th degree fit is seen to oscillate around the curve of lower degree, but the relative differences are small. For $x > 0.9$ the tensile force increases steeply, and both curves diverge. For a RW of 160 segments the results are presented in Figure 3. They are obtained in an analogous way, except for the fact that the fit function to the F_0/kT data for $0.1 \le x \le 0.9$ is of the fifth degree.

For very high extensions ($x \approx 1$) the results for the tensile force of RWs and SAWs *converge*. Analogous results are found for the other chain lengths studied ($19 \le n \le 159$; not shown). In Figure 4 we plotted the limiting tensile force at complete extension versus the chain length (results for SAWs and RWs are identical). We find that the tensile force at complete extension behaves as a scaling law in the number of steps n,

$$\frac{f_0(x=1)L}{kT} = -2.05n^{1.21} \qquad (2.2.1)$$

It seems that the tensile force at complete extension scales as $n^{2\nu}$, where ν (perhaps coincidentally) comes out

on the value of the Flory exponent for a SAW. (In the limit of large chain lengths the value of ν is about 0.59, but it is well-known that for lower values of n one finds slightly higher values.) We conclude that near complete extension, the RWs have a very small probability of intersecting themselves. As a result they adapt the behavior and, consequently, the exponent of SAWs.

Theoretical expressions for the end-to-end distribution function have been presented for RWs as well as for SAWs for the limit of large chain lengths. The former is well-known as the Gaussian distribution,

$$P_{\mathrm{G}}(\mathbf{R}) = \left(\frac{3}{2\pi n a^2}\right)^{3/2} \exp\left(-\frac{3\mathbf{R}^2}{2na^2}\right) \qquad (2.2.2)$$

the latter is known as the form of Des Cloizeaux,[19]

$$P_{\mathrm{DC}}(\boldsymbol{\rho}) = A\boldsymbol{\rho}^{\vartheta} \exp(-\beta\boldsymbol{\rho}^{\delta}) \qquad (2.2.3)$$

where $\boldsymbol{\rho}$ is the scaled end-to-end vector of the SAW ($\boldsymbol{\rho} = \boldsymbol{R}/an^{\nu}$) and the parameters have the values $A = 0.23$, $\beta = 1.045$, $\delta = 1/(1 - \nu) = 2.443$, $\nu = 0.591$, and $\vartheta = 0.275$. (Note that the parameter ϑ has no relation to θ-solvents.)

From these theoretical expressions one may calculate the reduced tensile force, by taking the natural logarithm and differentiating with respect to x ($= R/L = R/na$). One obtains for the reduced tensile force of a RW and a SAW, respectively, the following expressions

$$\left(\frac{f_0 L}{kT}\right)_{\mathrm{G}} = -3nx \qquad (2.2.4)$$

$$\left(\frac{f_0 L}{kT}\right)_{\mathrm{DC}} = \frac{\vartheta}{\mathrm{x}} - \beta\delta n x^{\delta-1} \qquad (2.2.5)$$

In Figures 2 and 3 we plotted the corresponding curves (dashes). For intermediate x values the fitted and theoretical results agree quite well. For RWs the exact curve for the cubic lattice and the theoretical limiting curve diverge for about $x \geq 0.6$, for SAWs this is the case for $x \geq 0.45$.

For small x values (for $x < 0.2$ for SAWs and for $x < 0.1$ for RWs, for all chain lengths studied) the fit curves and the theoretical results diverge. In this work this is of minor importance, as in the case of partially swollen gels the chains in the network are always rather extended, so that these low x values are never attained. We will therefore not study this aspect any further.

2.3. Electrostatic Contribution to the Tensile Force in the Network. For the electrostatic part of the free energy of a polyelectrolyte chain with fixed endpoints we derived two different expressions in part 1.[13] First we found an empirical fit equation, which covers in particular the simulation data at high charge densities (see eq 4.6 in part 1). Differentiating that expression with respect to R and taking the negative, we find

$$\frac{f_{\mathrm{q}} L}{kT} = -(n+1)A_1\left[\left(\frac{q}{n+1}\right)^2 + A_2\left(\frac{q}{n+1}\right) + A_3\right]C_1 \times \exp(-B_2\kappa a) \qquad (2.3.1)$$

The values of the parameters are given in Table 1.

Besides, we obtained expressions for the electrostatic contribution to the partition sum, by improving the corresponding result from Katchalsky's theory (see eqs 5.4a−c in part 1). These expressions agree well with the simulation results for moderate charge densities and are better understood from a theoretical point of view. Following the similar line of derivation leading to eqs 2.2.4 and 2.2.5 we obtain in this case the electrostatic contribution to the (reduced) tensile force. For less than two charges the result is zero. For two charges (located at both endpoints; $q = 2$) we find

$$\frac{f_q L}{kT} = \frac{Qe^{-\kappa R}}{R}\left(\kappa L + \frac{L}{R}\right) \qquad (2.3.2a)$$

and for more than two charges ($q > 2$) one obtains

$$\frac{f_q L}{kT} = \frac{Qe^{-\kappa R}}{R}\left(\kappa L + \frac{L}{R}\right) - \frac{(q-2)(q+1)}{2}\frac{L}{R} + \sum_{j=1}^{q-2}\frac{2(q-j)L}{(1-\xi)}\left\{\left[\int_0^\infty r \exp\left\{-\frac{Q}{r}e^{-\kappa R}\right\}\left[(r-\xi R)\times \exp\left(-\frac{(r-\xi R)^2}{\xi(1-\xi)}\right) + (r+\xi R)\exp\left(-\frac{(r+\xi R)^2}{\xi(1-\xi)}\right)\right] dr\right] \Big/ \left[\int_0^\infty r \exp\left\{-\frac{Q}{r}e^{-\kappa R}\right\}\left[\exp\left(-\frac{(r-\xi R)^2}{\xi(1-\xi)}\right) - \exp\left(-\frac{(r+\xi R)^2}{\xi(1-\xi)}\right)\right] dr\right]\right\} \qquad (2.3.2b)$$

where ξ is equal to $j/(q-1)$ and all lengths are scaled by h_0, the most probable value of the endpoint distance of the uncharged chain (approximated by $h_0^2 = (2/3)R_0^2$, which is strictly valid for Gaussian chains; R_0^2 is the mean square end-to-end distance of the chain). r is the spatial distance between two charged segments on the chain. Note that a positive sign denotes an expansive contribution.

In part 1[13] we found that the empirical fit equation (see eq 4.6 and Figure 6 in part 1) is more appropriate for high q values and that our variant of the expression of Katchalsky (eqs 5.4a−c and Figure 9 in part 1) better covers the simulation data for the electrostatic free energy contribution for lower q values. Studying the *derivatives* of the free energy expressions, being the tensile forces, one observes that, for small q values and moderate extensions, the slope of our Katchalsky variant agrees well with the corresponding slope of the simulation data. For high q values and large extensions the simulation curves are somewhat steeper than our variant of Katchalsky's expression predicts, whereas the empirical fit curves for F_q/kT are somewhat steeper (as a function of R) than the simulation curves.

Table 1. Values of the Coefficients in the Expression (2.3.1) for f_q, the Electrostatic Contribution to the Tensile Force Exerted by a Lattice Polyelectrolyte with Fixed End Points, for $\kappa a \geq 0.3$, for $0.1 \leq q/(n+1) \leq 0.5$ and $0.3na \leq R \leq na$ (cf. Part 1[13])

coefficient	$n = 9$	$n = 19$	$n = 39$	$n = 79$
A_1	15.3	16.0	17.4	20.3
A_2	−0.34	−0.23	−0.20	−0.20
A_3	0.029	0.013	0.011	0.010
B_2	1.39	1.62	1.77	1.89
C_1	0.65	0.65	0.65	0.65

This indicates that for small q values the Katchalsky variant will give more accurate results for the tensile force (and thus for the gel behavior), whereas for high q values the outcomes from the simulation results will lie somewhere between both descriptions, but closer to the empirical fit description.

2.4. Network Pressure. To calculate the pressure exerted by the network, the area on which the perpendicular component of the tensile force acts must be determined. This area depends on the precise network structure, on the functionality of the cross-links, and on the concentration of the chains. Assuming tetrafunctional cross-links, and a "perfect" tetrahedral arrangement of the polyions (see Figure 1), it can be shown[20] that the network pressure exerted by the polyions is given by

$$\frac{\Pi_{\text{network}}}{N_A kT} = \frac{3^{1/2}}{4}\frac{1}{N_A L^3 x^2}\left(\frac{f_0 L}{kT} + \frac{f_q L}{kT}\right) \qquad (2.4.1)$$

where the combination $N_A k$ is equal to the gas constant, often denoted by R. However, here we have reserved the symbol R to denote the end-to-end distance (vector) of the chain.

2.5. Donnan Osmotic Pressure Difference. This contribution, denoted $\Delta\Pi_{\text{Donnan}}$, is the net (expansive) osmotic pressure difference between the internal solution in the gel and the surrounding medium,

$$\Delta\Pi_{\text{Donnan}} = \Pi_{\text{inner}} - \Pi_{\text{outer}} = N_A kT(\varphi_p q C_p + 2C_s - 2C_e) \quad (2.5.1)$$

where C_p is the concentration of polyions and q is the number of charges per polyion, so that qC_p is the maximum number of counterions that can be released from the polyion into the inner solution. φ_p is the osmotic coefficient of the counterions, here defined according to Manning's condensation theory,[21]

$$\varphi_p = 1 - \frac{1}{2}\lambda \quad \text{for} \quad \lambda \le 1, \quad \text{and} \quad \varphi_p = \frac{1}{2\lambda} \quad \text{for} \quad \lambda > 1$$

where λ is the charge parameter, defined as $\lambda \equiv qQ/L$. Counterion condensation, which occurs for $\lambda \ge 1$ and which results in a lowering of the effective charge on the polyion and a reduced osmotic activity of the counterions present, is thus taken into account, following the line charge concept of Manning. In this concept the deviation of φ_p from unity reflects the interactions of the small ions with an infinitely long line charge. Contributions from the interaction between small ions and from the interaction between different polyions are neglected (see ref 2 for a detailed discussion on the derivation). C_e is the external concentration of monovalent (1−1) salt and C_s is the salt concentration in the gel. All concentrations are in moles per meter cubed.

Due to the presence of the polyions in the internal solution, the salt ions that try to penetrate the gel from the external solution are partially expelled from the interior of the gel (Donnan exclusion). The equation describing this phenomenon is (see ref 2 for a detailed discussion on the derivation and Manning's result)

$$C_s(C_s + qC_p) = C_e^2 G_D^2 \qquad (2.5.2)$$

G_D^{-1} denotes the activity coefficient of the salt ions *in* the gel, relative to their activity coefficient in the surrounding solution,[21]

$$G_D^{-2} = \exp\left\{-\frac{\lambda q C_p}{qC_p + 2C_s}\right\} \quad \text{for} \quad \lambda \le 1 \qquad (2.5.3a)$$

$$G_D^{-2} = \left(\frac{\frac{qC_p}{\lambda} + C_s}{qC_p + C_s}\right)\exp\left(-\frac{qC_p}{qC_p + 2C_s\lambda}\right) \quad \text{for} \quad \lambda > 1 \qquad (2.5.3b)$$

Note that the set of eqs 2.5.2 and 2.5.3 must be solved iteratively, to obtain the equilibrium values of C_s. The value for C_s is then also used to calculate the inverse Debye screening length, κ, *in* the gel,

$$\kappa^2 = 4\pi Q N_A(2C_s + qC_p) \quad \text{for} \quad \lambda \le 1$$

$$\kappa^2 = 4\pi Q N_A\left(2C_s + \frac{qC_p}{\lambda}\right) \quad \text{for} \quad \lambda > 1 \qquad (2.5.4)$$

Explicit expressions for $\Delta\Pi_{\text{Donnan}}$ (involving the chain length, the external salt concentration, the number of charges on the chain, and its relative extension) can easily be derived if the ("ideal") gel structure is known. For our model calculations we use (cf. Figure 1)

$$C_p = \frac{2}{N_A\left(\frac{2na}{3^{1/2}}\right)^3 x^3} = \frac{3^{3/2}}{4}\frac{1}{N_A(na)^3 x^3} \quad (\text{in mol/m}^3) \qquad (2.5.5)$$

For every value of C_e, q, and x, the value of C_s can be found iteratively from Eqs 2.5.2 and 2.5.3. Using the values of C_e, q, C_p, and C_s thus obtained, one finds $\Delta\Pi_{\text{Donnan}}$ and κ.

2.6. Osmotic Pressure Contribution Due to Mixing Polymer and Solvent. For the last contribution, Π_{mix}, which contains the contribution from the dissolving polymer molecules themselves, including the interaction of the polymer with the solvent (expressed in terms of the interaction parameter χ), we use the well-known result of Flory−Huggins[6]

$$\frac{\Pi_{\text{mix}} V_w}{N_A kT} = -(\ln(1-\phi) + \phi + \chi\phi^2) \qquad (2.6.1)$$

where V_w is the molar volume of the solvent (water), equal to 18×10^{-6} m^3. For our model calculations we use

$$x^3 = \frac{V}{V_{\max}} = \frac{\phi_{\min}}{\phi} \Rightarrow \phi = \frac{\phi_{\min}}{x^3} \quad \text{where}$$

$$\phi_{\min} = \frac{3^{3/2}}{4}\frac{nV_m}{N_A(na)^3} \qquad (2.6.2)$$

Here $\phi_{\min}$ is the minimum value of the volume fraction of the polyelectrolyte, attained at complete extension of the chains.

3. Results

3.1. General. In this section we present the results found for the swelling behavior of a model polyelectrolyte gel, consisting of tetrahedrally ordered, cross-linked lattice polyelectrolyte chains. This is done by determining the relative extension x of the chains for which the

Table 2. Conversion Factors for Calculation of Swelling Ratios with Respect to Different Reference Volumes

	SAW		RW	
n	V_{min}/V_{max}	V_{min}/V_0	V_{min}/V_{max}	V_{min}/V_0
39	0.0622	15.0	0.0169	4.08
79	0.0293	29.3	0.00569	5.70
159	0.0131	53.3	0.00195	7.94

total (osmotic) pressure of the gel equals zero ($\Pi = 0$; see eq 2.1.1). With the obtained value of x the swelling volume can then be found.

In the figures presented, the degree of swelling is defined as the actual equilibrium volume (V) of the gel, relative to its minimum swelling volume at very high external salt concentrations: V/V_{min}. The latter, V_{min}, is effectively equal to the swelling volume of the same gel in the uncharged state, as at very high salt concentrations the charge interactions are completely screened. We used this reference volume, as it gives direct insight into the magnitude of the collapse of the gel upon addition of salt. For a comparison of the swelling results presented, the reader might prefer a different reference volume, e.g., V_0 or V_{max}. Table 2 contains the factors needed for this conversion.

In some experimental situations, however, the swelling state at high salt concentration, corresponding to V_{min}, might not be attainable, as the solvent quality usually depends on the ionic strength. At very high salt concentrations, the solvent might even become so strongly polar, that the polyelectrolyte precipitates ("salts out"). In this paper only both limiting cases where the polymer is still soluble ((athermal) good and θ-solvent) are studied, and the change of solvent quality with salt concentration is not taken into account.

Part of the results are presented in terms of linear charge densities, defined as $q/(n + 1) \times 100\%$, for values of the linear charge density up to the counterion condensation threshold, which, according to Manning's theory, limits the effective linear charge density to 35%.

First we study the difference in swelling behavior obtained using both descriptions for the charge contribution to the tensile force (eqs 2.3.1 and 2.3.2), for a gel of short chains (40 segments). Then we show the behavior of a gel of longer chains, using the general expression for the bare tensile force of SAW chains (presented in the Appendix) and introducing the electrostatic interactions by means of our Katchalsky variant (2.3.2). This gel, which can be interpreted as a polyelectrolyte gel in a good solvent, is then compared to a similar gel composed of charged RWs, a model for the same polyelectrolyte gel, but now submerged in a θ-solvent. For the latter model we use the tensile force exerted by a RW (see the Appendix) and our Katchalsky variant for the charge interactions in which the parameter values are adapted to the RW values. We did not perform direct MC calculations on RW chains with fixed endpoints. Some characteristic differences in the behavior of the model gel, for both (limiting) solvent conditions, are discussed. Next we compare our predictions with experimental results. Finally, we investigate the different contributions to the osmotic pressure of the gel for both solvent cases.

For consistency, in all figures and calculations presented for either SAW chains (good solvent) or RW chains (θ-solvent), the values of the relevant parameters were adapted to either case: the χ-parameter was set to 0 and 0.5, respectively,[22] and h_0^2 was given a value of $(2/3)\langle R_0^2\rangle$, for both the SAW and the RW chain under consideration (see Table 3 in part 1[13]).

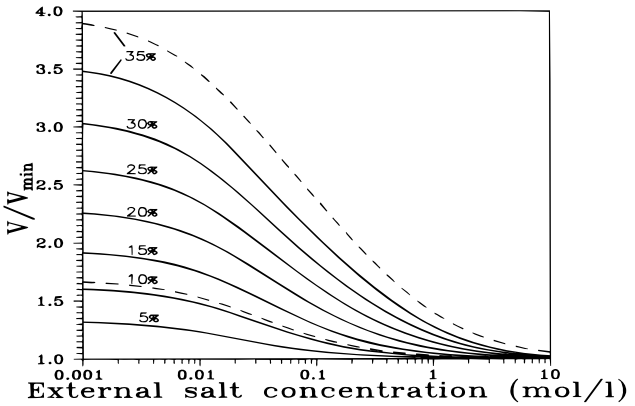

Figure 5. Equilibrium degree of swelling (V/V_{min}) of a gel consisting of SAW lattice polyelectrolyte chains of 40 segments, versus the salt concentration C_e in the surrounding medium, for different values of the linear charge density (indicated in the figure). For the tensile force of the bare chains a direct fit to the simulation data for $n = 39$ was taken. For the electrostatic contribution we took the empirical fit (eq 2.3.1, solid curves). For comparison the swelling curves obtained from our modified expression of Katchalsky are also plotted (eqs 2.3.2a,b, dashed curves) for 10% and 35% linear charge density.

3.2. Simple Gel of Short Chains, Described Only by Monte Carlo Simulations. In Figure 5 we plotted the equilibrium degree of swelling, V/V_{min}, of the gel consisting of SAW chains of 40 segments, versus the external salt concentration, for various linear charge densities, using the empirical fit expression (eq 2.3.1) to account for electrostatic interactions. One can observe that this gel swells only moderately: even for high values of the linear charge density the maximum volume is only about 3 times its value without charges. This is an implication from taking the good solvent limit, as will be discussed in section 3.3.

In the figure we also plotted the calculated swelling curves (dashed curves), using our Katchalsky variant (eqs 2.3.2) for the electrostatic contribution to the network pressure, for 10% and 35% linear charge density. The curves show that for chains of 40 segments the difference in the degree of swelling (obtained by using either eq 2.3.1 or 2.3.2) is at most 15%, assuming that counterion condensation limits the linear charge density to 35%.

As discussed in section 2.2, a comparison of (a) the derivatives of the simulation results, (b) the empirical fit expression, and (c) our Katchalsky variant suggests that the "exact" swelling curve (if it could be derived from the simulation data directly) would lie somewhere between both plotted curves.

For moderate q values the exact swelling curve would lie near the results of our Katchalsky variant. For high charge densities our Katchalsky variant becomes less accurate and the exact swelling curves would lie more closely to the results from the empirical expression.

3.3. Gels of Longer Chains. To study the behavior of gels of longer chains ($n > 40$), we use the expressions for the tensile force of the bare chain as a function of the relative extension, as given in the Appendix. For SAW chains this means that we use an extrapolation. For RW chains we use a 5th degree fit to the exact distribution function for every chain length used. As for chains longer than 40 segments we have much less (n

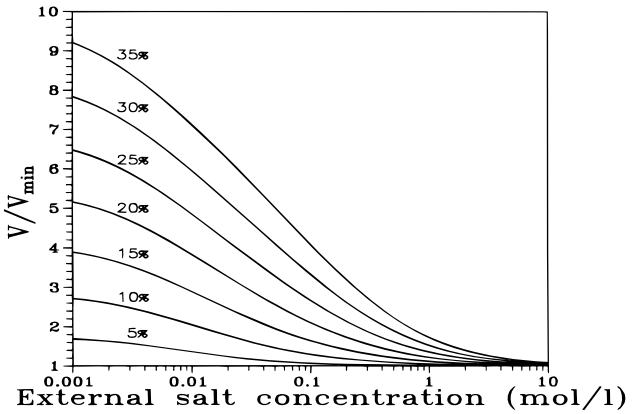

Figure 6. Equilibrium degree of swelling of a gel of charged SAW chains of 80 segments versus the external salt concentration. Plotted are the results for different values of the linear charge density (indicated in the figure).

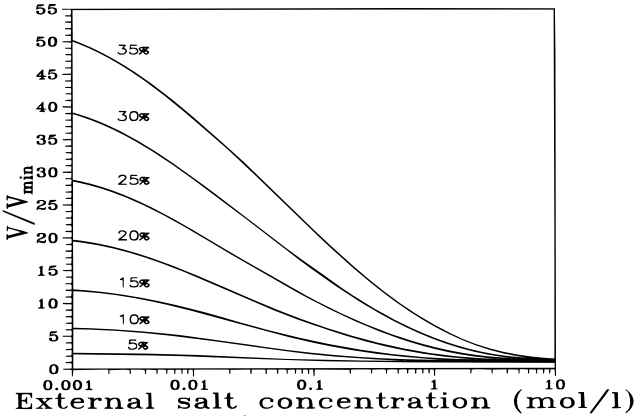

Figure 7. Similar plot as Figure 6, but now for RW chains.

= 79) or no (n > 79) accurate MC data for the electrostatic contribution, the validity of the empirical expression becomes questionable. For these cases we therefore employ our Katchalsky variant (eq 2.3.2), for which we have theoretical support. In doing so we assume that maximum relative errors in the results still will be more or less of the same order of magnitude as found for chains of 40 segments (15%; see Figure 5, where we maintain the assumption that counterion condensation limits the effective charge density to 35%).

In Figure 6 we plotted the equilibrium degree of swelling of gels of charged SAW chains of 80 segments versus the external salt concentration (i.e., the swelling behavior of a polyelectrolyte gel in a good solvent). Figure 7 shows the same plots for RW chains (i.e., for a polyelectrolyte gel in a θ-solvent).

At first sight, the gel in θ-solvent seems to swell to a much larger extent than the gel in good solvent (see Figures 6 and 7). However, if we plot (in Figure 8), for both types of solvent, the relative extension of the chains as a function of the external salt concentration, one observes that the large difference is mainly caused by the stronger contractive properties of the gel in θ-solvent. In other words: the gel composed of RWs has a much smaller value of V_{min}, so that the degree of swelling is much larger. One sees that in the case of high charge (30%) and low external salt concentration (and therefore strong charge interactions) the gels consisting of RW chains and SAW chains show almost the same relative extension, so that the swelling ratio with respect to V_{max} is more or less the same in both

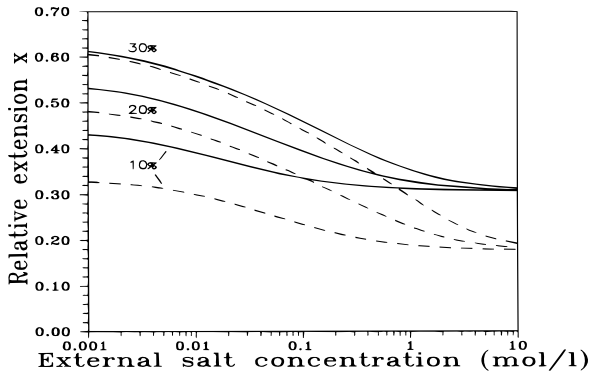

Figure 8. Relative extension of charged SAW chains (solid curves) and of charged RW chains (dashed curves) of 80 segments, incorporated in a gel which is submerged in a salt solution, versus the salt concentration, for different linear charge densities on the network chains (indicated in the figure).

cases. At high linear charge densities self-intersection of the RWs is very unlikely, due to the strong charge interactions, so they behave more or less like SAWs. Second, at high degrees of swelling the influence of the mixing term, which is also different for both cases, must be relatively small (the magnitude of this term is driven by the mixing opportunities that still exist for the system, and these are small at high swelling). Furthermore, at these high extensions the influence of the difference in h_0 values of both types of chains appears to be relatively small.

Adding salt or decreasing the linear charge density means that in the case of RWs the "self-avoiding" behavior induced by the strong charge interactions disappears; as a result the collapse of these self-intersecting chains is stronger. This is also reflected in their tensile force, which is generally higher than in the case of SAWs (compare, for instance, Figures 2 and 3). Another cause of the stronger contractive behavior of gels of RWs is the fact that the mixing term, favoring swelling, is less important in that case.

Comparing the swelling results of gels of tetra- and hexafunctionally cross-linked chains of the same length and under further equal conditions, we observe that the denser gels (with hexafunctional cross-links) show smaller swelling ratios on both ends of the deswelling curve (not shown). Apparently, at low salt concentrations the higher osmotic pressure from the counterions is more than compensated by the higher contractive network pressure (caused by more chains per unit volume and the neglect of interchain electrostatic interactions). At high external salt concentrations the larger mixing term prevents the denser gels from shrinking strongly.

In Figure 9 the other cross-section of the data is shown: the equilibrium degree of swelling of similar gels as a function of the linear charge density, for different chain lengths, at a constant external salt concentration of 0.1 mol/l, both in good and θ-solvent. Over the entire q range the resulting curves can be well described by using quadratic functions in q. This differs from scaling predictions.[4,12,23] Furthermore we find that up to a charge density of 20% the degree of swelling V/V_{min} and the chain length n show a perfect linear relationship. This also differs from scaling predictions.[4,12,23]

For higher q values and shorter chains ($n \leq 39$) for which we do know the values of the fit parameters, the

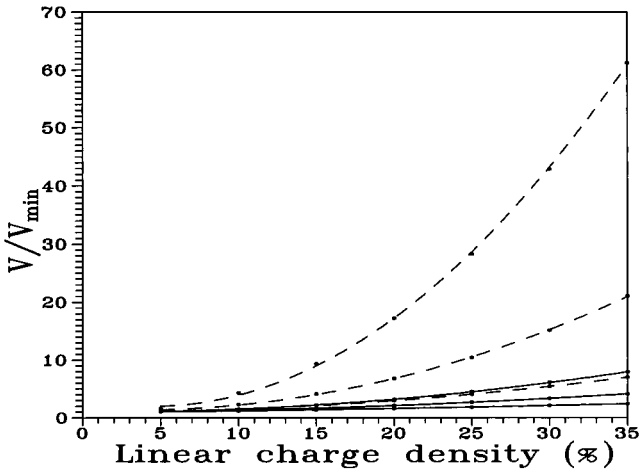

Figure 9. Equilibrium degree of swelling of a gel of charged SAW chains (good solvent; solid curves) and charged RW chains (θ-solvent; dashed curves) versus the linear charge density, for chains of 40 (lowest solid and dashed curves), 80 (intermediate solid and dashed curves), and 160 segments (upper solid and dashed curves), at a constant external salt concentration of 0.1 mol/L. The curves are best fit parabola to the indicated data points. For the electrostatic contribution to the network pressure eqs 2.3.2a,b are used.

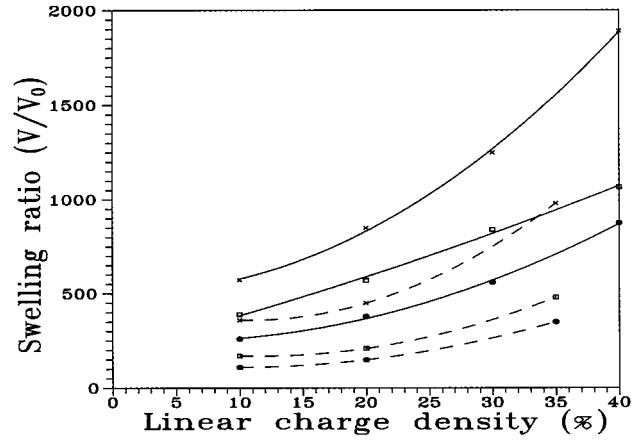

Figure 10. Experimental values of Skouri et al.[24] for the swelling ratio of PAA gels versus the linear charge density. V is the equilibrium swelling volume; V_0 the *dry* gel volume. Results are shown for different degrees of cross-linking agent (solid lines, 1%; dashed, 2%) and for different external salt concentrations: (x) 0 mol/L; (□), 0.2 mol/L; and (●) 0.5 mol/L. The plotted curves are best fit parabola to the data points.

empirical fit expression (2.3.1) must be used for the electrostatic contribution to the tensile force. For those cases we also find a quadratic dependence on q and a linear dependence on n (not shown).

We conclude that at a fixed external salt concentration and for the n and q values studied, the equilibrium degree of swelling is a quadratic function of q and is linearly dependent on n.

In Figure 10 we plotted results of Skouri et al.[24] for the equilibrium swelling ratio of PAA gels as a function of the linear charge density, for two values of the cross-link density and for three values of the external salt concentration. Note that the *swelling ratio* is defined as V/V_0 instead of V/V_{min} (=*degree* of swelling). The curves plotted are best-fit parabola to the data points. Except for the data for 1% cross-link density and 0.2 mol/L salt concentration, the experimental results show the same qualitative behavior as our theoretical results (Figure 9). The linear dependence on the chain length

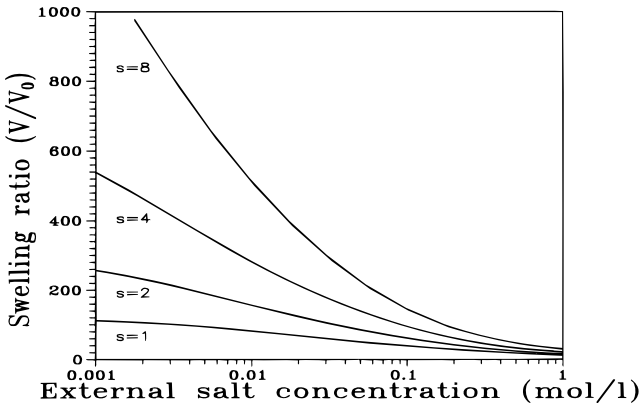

Figure 11. Swelling ratio of a model gel of RW chains of 80 segments as a function of the external salt concentration, for different values of the Kuhn segment length (indicated in the figure; s is the number of chain segments per Kuhn segment). The linear charge density is 20%. Note that for a proper comparison with the experimental results the *swelling ratio* (defined as V/V_0, the equilibrium swelling volume relative to the *dry* volume of the gel) is shown.

cannot be verified unambiguously for real gels, because of the defects mentioned in the Introduction. However, as far as a simple comparison is allowed, also the linear dependence on chain length agrees well with our predictions.

3.4. Quantitative Comparison with Experimental Values. When making the comparison between our theoretical results for the swelling ratio and the experimental values of Skouri, we find that our results are about 1 order of magnitude lower than the experimental values. This discrepancy is due to the high flexibility of the uncharged model chains. This causes the tensile forces of the model chains to be too strong, so that a gel of these chains swells too little as compared to the real system.

To correct for this difference in intrinsic stiffness of the bare chains, we consider the wormlike chain (WC) model.[25] In the limit of long chains, the WC becomes equivalent to a RW, the effective Kuhn length of the RW (equal to its step length) being equal to twice the persistence length of the WC. Denoting the number of lattice chain segments per Kuhn segment by s, we now rescale the RW to consist of n/s steps of length sa, to decrease its flexibility. Note that only RWs with an integer number of steps make sense, so n/s must be an integer. We calculated the deswelling curves for a gel of RW chains of 80 segments, for different values of s. The bare tensile force is described by that of a RW of n/s steps, and the value of h_0 is adapted to the smaller number of longer Kuhn segments: $h_0^2 = (2/3)Lsa$. The results are shown in Figure 11 and can be compared to the experimental values found for a PAA gel, shown in Figure 12.

The persistence length of PAA (in the almost uncharged, acid form) is about 10 Å, so that the length of its Kuhn segments is about 20 Å, i.e., the length of about eight steps of the lattice RW. The comparison shows that indeed for $s = 8$ the calculated degree of swelling falls into the same range as the measured values. Besides, the salt concentration dependence of the swelling ratio is described much more satisfactorily. Note that by using chains of 80 segments we assumed that about one-third of the added cross-linking agent (2%) is actually built into the network structure.

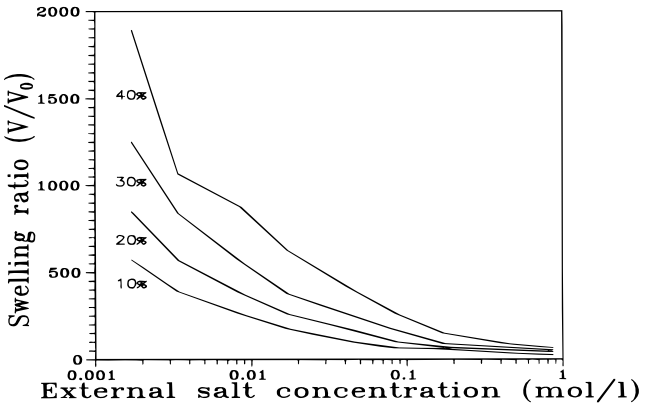

Figure 12. Experimental values[24] for the equilibrium *swelling ratio* (V/V_0) of a PAA gel versus the external salt concentration, for different values of the linear charge density (indicated in the figure). The cross-link density is 2%. The straight lines connecting the data points are added as a guide to the eye. For clarity symbols indicating the data points are not shown.

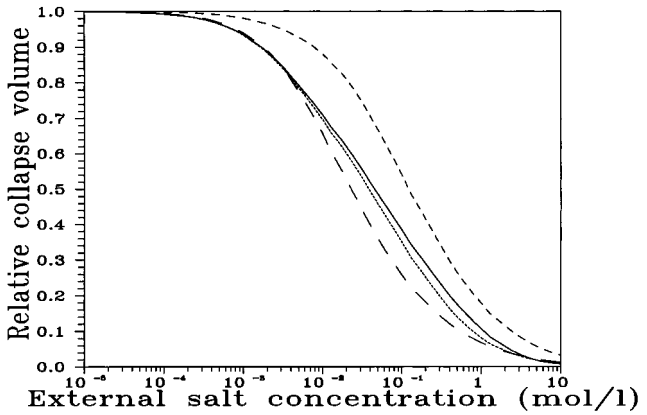

Figure 13. Relative collapse volume, $((V/V_{min}) - 1)/([V/V_{min}]_{C_e=0.00001} - 1)$ (see text), versus the external salt concentration C_e, showing the onset and the rapidity of the course of the collapse of four different gel types. Plotted are curves for gels of fully charged (35% charge density) chains of 80 segments: semiflexible chains (short dashes, ref 2), charged SAW chains (solid curve), charged RW chains (dotted curve) and the original gel model of Katchalsky (long dashes, refs 2 and 11).

Note that for SAW chains a simple rescaling of the Kuhn segment length cannot be performed so easily as for RW chains, as a rescaling of the Kuhn segment length also affects the lateral dimension of the segments, which is not desired. However, an adaptation of the Kuhn segment length of SAW chains can be done by performing more sophisticated Monte Carlo simulations, employing "correlated self-avoiding walks", the persistence length of which can be adapted without altering the segment and/or chain dimensions.

3.5. Comparison to Some Other Theories. To get another perspective on the deswelling and collapse of the model gel upon addition of salt in the external medium as compared to the other gel models mentioned, we plotted, in Figure 13, the "relative collapse volume", V_{rc}, defined by

$$V_{rc} = \frac{(V/V_{min}) - 1}{(V/V_{min})_{C_e=0.00001} - 1} \qquad (3.5.1)$$

versus the external salt concentration C_e (in moles per liter). By plotting the swelling data this way, every gel type shows a collapse from an initial value of one to a final value of zero (attained at very high external salt concentration; not shown). Relative differences in the collapse behavior (like the onset of the collapse, the rapidity of the collapse and the concentration range over which the collapse occurs) are thus conserved and made comparable. The plot shows the collapse behavior of gels consisting of different types of tetrafunctionally cross-linked chains of 80 segments: semiflexible chains, SAW chains, RW chains, and the chains in Katchalsky's original gel model[11] (see also ref 2).

One observes that the onset of the collapse of the semiflexible chains occurs at higher C_e values than where the gels of the other (much more flexible) chains begin to deswell. This is due to the chains' high intrinsic stiffness, induced by their incomplete conformational statistics.[2] Near a complete extension this causes their tensile forces to strongly decrease upon a slight decrease of the relative extension. Therefore a strong salt concentration increase is needed for the onset of the collapse to take place.

Further, the onset of the collapse of the original gel model of Katchalsky and of our modified model occurs at the same external salt concentration. This indicates—although the description is somewhat different[2] —that the Donnan contribution is accounted for more or less in the same way. At higher salt concentrations the charge interactions on the chain's backbone are screened and differences in the conformational statistics of the chains become apparent. In Katchalsky's model the chain statistics are assumed to be Gaussian, even in their charged state. The charged segments are therefore allowed to intersect themselves as much as if they were *not* charged. As a result the contribution from the charge interactions to the total free energy of the chain is much larger than in the case of the other models. Conversely, adding salt has therefore also a much stronger impact on the interactions between the segments in these chains and thus results in a much stronger collapse behavior than observed in the other chain models.

One can see that halfway the deswelling range the relative differences between the three descriptions are more or less the same. The relative difference between the deswelling curve of the gel of stiff, semiflexible chains and of our model gel is comparable to the relative difference between the deswelling curve of our model gel and of Katchalsky's model gel, which contains far too flexible chains. This shows that the increase in chain stiffness, caused by a correct incorporation of charge interactions in Katchalsky's model, is just as substantial as the difference between the semiflexible (semicircular) chains and the much more flexible lattice chains.

3.6. Osmotic Pressure Contributions in Swelling Equilibrium. To understand better the swelling processes that occur in the model gels of flexible polyelectrolyte chains studied here, we now focus on the different contributions to the osmotic pressure, their relative importance, and the changes therein while deswelling the gels in a salt solution of increasing ionic strength. In Figures 14 and 15 we plotted the four contributions to the reduced osmotic pressure ($\Pi V_w/N_A kT$) in the gel: the contractive pressure exerted by the uncharged chains, the expansive contribution from the network charges, the Donnan osmotic pressure difference between the inner and outer solution, and the osmotic mixing term, both for gels of SAW chains and

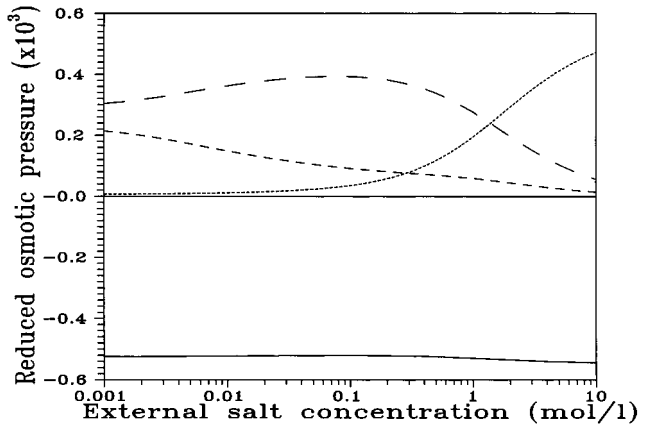

Figure 14. Comparison of the four contributions to the osmotic pressure in a gel of fully charged (35% linear charge density) SAW chains of 80 segments, versus the external salt concentration. Plotted are the contractive pressure exerted by the uncharged chains (solid curve, eq A.1 with eq 2.4.1), the contribution from the charges (long dashes, eqs 2.3.2a,b with 2.4.1), the Donnan osmotic pressure difference between the inner and outer solution (short dashes, eq 2.5.1), and the mixing contribution (dotted curve, eq 2.6.1).

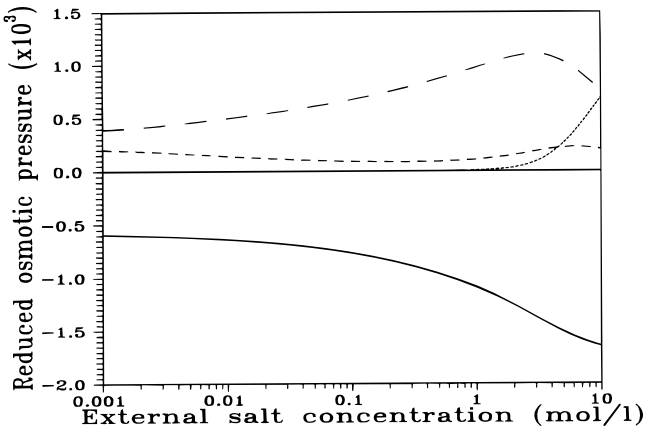

Figure 15. Same as Figure 14, but now for a gel of RW chains. Equation A.2 is taken for the bare chain contribution.

of RW chains, i.e., for swelling in a good and a θ-solvent. Note that all contributions are related to each other through the variable x. In swelling equilibrium the value of x is chosen such that the total osmotic pressure in the gel is zero (cf. eq 2.1.1.).

For both cases the figures show that the *pressure exerted by the bare network* is negative (i.e., contractive) and compensates for the effect of the other three, expansive, contributions. An interesting aspect is that in the deswelling process the pressure exerted by the bare network does not strongly decrease (in an absolute sense), as is the case for semiflexible chains,[2] although the curve for good solvent conditions shows a very slight indication of such a decrease around salt concentrations of 0.1 mol/L. Overall, in the good solvent case, the bare network pressure remains more or less constant, indicating that, while the gel is deswelling and the network contracting, the decrease of the bare network force is of roughly the same magnitude as the reduction of the area on which the force acts. This is clear from Figure 2 (where $f_0 \sim x^2$). As the network pressure is proportional to f_0/x^2, the pressure exerted by the bare network remains more or less a constant. The bare network pressure in a θ-solvent shows a different behavior for increasing salt concentration. In this case the bare network pressure *increases* strongly, as for this type of chains $f_0 \sim x$ (see Figure 3) and the area on which f_0 acts is proportional to x^2, so that the network pressure is more or less proportional to $1/x$. This causes the strong absolute increase of the bare network pressure at high salt concentrations (i.e., at small degrees of swelling and therefore at small values of x).

While salt is added and the gel shrinks, the charges on the chain approach each other, giving rise to an increase of the *pressure contribution from the charge interactions along the chains*. At the same time, due to this addition of external salt, the ionic strength in the gel increases, so that the charge interactions are screened more effectively. At some finite salt concentration both effects cancel, which gives the maximum in this pressure contribution. In the case of RW chains the gel shows a stronger contraction, so that the interactions between charges persist until higher salt concentrations. This results in a shift of the position of this maximum toward higher salt concentrations, as compared to the SAW case.

Generally, the addition of salt in the external solution causes more salt ions to penetrate the gel. As a result of this effect the *Donnan osmotic pressure difference between the inner and outer solution* decreases, and the gel shrinks. Due to their nature, the RW chains show a stronger collapse than the SAW chains, which apparently leads, at higher salt concentrations, to such a strong increase of the counterion concentration that in the RW case a small maximum in this contribution is reached at a certain, finite, high external salt concentration. Clearly, this maximum occurs at a salt concentration higher than where the electrostatic pressure contribution has its maximum value, i.e., at salt concentrations where the charge interactions are strongly decreasing and where the gel thus collapses strongly.

The osmotic pressure contribution from mixing polymer and solvent is predicted by eq 2.6.1. The good and θ-solvent case show a large difference. In the case of RW chains the ϕ and ϕ^2 contributions to this pressure term are zero, and the higher order contributions, originating from three and more particle interactions, play a part at high volume fractions of the polymer. Obviously, the mixing term vanishes at low volume fractions, which can be seen by expanding eq 2.6.1 and substituting $\chi = 0.5$: up to order ϕ^2 all terms vanish. For the SAW case (good solvent, $\chi = 0$), there is still a ϕ^2 contribution, due to the binary excluded volume interaction of the segments. Therefore, at very high degrees of swelling, and thus for small values of ϕ, the mixing term may still contribute to the osmotic pressure. At high external salt concentrations the situation is reversed; the gel of RW chains contracts stronger, therefore reaches higher values for ϕ than are attained in the good solvent case, and consequently this term gives a larger contribution to the osmotic pressure.

4. Conclusions

The network model presented in this paper can be used to predict, at least qualitatively, the swelling of a real polyelectrolyte gel as a function of the salt concentration in the surrounding fluid and of the linear charge density of the constituent chains. Two limits of solvent quality have been studied, i.e., a θ-solvent and a good solvent, referring respectively to charged RWs and to charged SAWs, both being the lattice chains that may

constitute the network. Chain−chain interactions are described only by the Flory−Huggins mixing term of the osmotic pressure, which becomes important at very high salt concentrations. For the remaining the model is valid as long as intrachain electrostatic interactions prevail. This situation is favored for highly swollen gels, e.g. at dilute salt concentrations and moderate, fixed linear charge densities.

Compared to the charged gel theory of Katchalsky, progress has been made in estimating the effects of intrachain electrostatic repulsions. In Katchalsky's approach the Gaussian segment distribution is assumed to be unaffected by the electrostatic interactions, whereas in our model a first-order perturbation in this distribution has been taken into account. As a result our model predicts a less drastic collapse of the gel with increasing salt content. Obviously our model should be improved further by including higher-order intrachain charge interactions and the electrostatic repulsions between different chains.

In our model SAWs and RWs tend to the same degree of expansion in the regime of low salt concentration and high linear charge density. However, with increasing salt content the RW network shows the most pronounced collapse, which, however, remains still an order of magnitude smaller than the deswelling of a PAA gel. This discrepancy originates from a mismatch of the lattice step length and the real chains' Kuhn segment length. In fact the bare lattice chains are much more flexible than their real equivalents. In the case of a PAA gel, theory and experiment can be reconciled by taking the Kuhn segment length equal to eight lattice steps. This implies that the lattice step of 0.25 nm is rescaled to 2.0 nm, being the Kuhn segment. The latter value is indeed about twice the bare persistence length of PAA.

In conclusion, the RWs are found to work quite well in the model, provided they are adapted to the correct persistence length. This agrees with the fact that some types of polyelectrolyte gels, in particular PAA, have a so-called "salting-out" behavior: at rather high salt concentrations these systems arrive at θ-conditions. Therefore, both for low and high salt contents the model employing RW chains gives results which compare semiquantitatively to those of real PAA gels.

Acknowledgment. Th.M.B. acknowledges support by the Koninklijke/Shell Laboratories, Amsterdam.

Appendix

In this Appendix we present the results for the fit curves obtained for the bare tensile force exerted by SAW chains and RW chains.

Results for SAW Chains. For SAW chains we obtained the following fit curve for the bare tensile force

$$\frac{f_0 L}{kT} = -n[a_2x^2 + a_1x + a_0] - [b_2x^2 + b_1x + b_0] \quad \text{(A.1)}$$

Where the coefficients have the following values

index i	a_i	b_i
0	0.3610	−15.923
1	−1.4929	75.380
2	5.6933	−83.793

Results for RW Chains. For RW chains we used the following fit curve for the bare tensile force (cf. Appendix 1 of part 1[13]).

$$\frac{f_0 L}{kT} = -(5a_1x^4 + 4a_2x^3 + 3a_3x^2 + 2a_4x + a_5) \quad \text{(A.2)}$$

where, for the values of n used, the coefficients are given by

n	a_1	a_2	a_3	a_4	a_5
9	0	2.470	-3.513	13.629	-0.269
19	12.623	−19.916	12.960	22.997	0.527
39	62.582	−115.35	82.233	31.447	3.082
79	189.27	−363.35	263.76	35.054	9.703
159	456.11	−887.87	648.25	35.555	23.748

References and Notes

(1) De Rossi, D.; Kajiwara, K.; Osada, Y.; Yamauchi, A. *Polymer Gels*; Plenum: New York, 1991. Many other examples are given in: *Adv. Polym. Sci.* **1993**, *110*.
(2) Barenbrug, Th. M. A. O. M.; Smit, J. A. M.; Bedeaux, D. *Polym. Gels Networks* **1995**, *3*, 331.
(3) Dobrynin, A. V.; Colby, R. H.; Rubinstein, M. *Macromolecules* **1995**, *28*, 1859.
(4) Rubinstein, M.; Colby, R. H.; Dobrynin, A. V.; Joanny, J.-F. *Macromolecules* **1996,** *29*, 398.
(5) Barrat, J.-L.; Joanny, J.-F. *Adv. Chem. Phys.* **1996**, *94*, 1.
(6) Flory, P. J. *Principles of Polymer Chemistry*; Cornell University Press: Ithaca, NY, 1953.
(7) Ohmine, I.; Tanaka, T. *J. Chem. Phys.* **1982**, *77*, 5725.
(8) Hill, T. L. *J. Chem. Phys.* **1952**, *20*, 1259.
(9) Ricka, J.; Tanaka, T. *Macromolecules* **1984**, *17*, 2916.
(10) Katchalsky, A. *J. Polym. Sci.* **1951**, *7*, 393.
(11) Katchalsky, A.; Lifson, S. *J. Polym. Sci.* **1953**, *11*, 409.
(12) Katchalsky, A.; Michaeli, I. *J. Polym. Sci.* **1955**, *15*, 69.
(13) Barenbrug, Th. M. A. O. M.; Smit, J. A. M.; Bedeaux, D. *Macromolecules* **1997**, *30***,** 605 (part 1).
(14) Ilavsky, M. *Polymer* **1981**, *22*, 1687.
(15) Hasa, J.; Ilavsky, M.; Dusek, K. *J. Polym. Sci.; Pol. Phys. Ed.* **1975**, *13*, 253.
(16) Hasa, J.; Ilavsky, M. *J. Polym. Sci.; Pol. Phys. ed.* **1975**, *13*, 263.
(17) Ilavsky, M. *Adv. Pol. Sci.* **1993**, *109*, 173.
(18) Barenbrug, Th. M. A. O. M.; Smit, J. A. M.; Bedeaux, D. *Macromolecules* **1993**, *26*, 6864.
(19) Des Cloizeaux J., Jannink G. *Les Polymeres en Solution*; Les Editions de Physique: Les Ulis, France, 1987.
(20) A derivation for a cubic arrangement of the polyions is given in ref 2 (eq 3.2). Choosing a tetrahedral structure changes only the prefactor into $3^{1/2}/4$.
(21) Manning G. S. *J. Chem. Phys.* **1969**, *51*, 924.
(22) Theoretically the χ-parameter of a polymer in a good (athermal) solvent adopts a value of zero. In practice one usually finds for this parameter values of 0.4−0.5. In this work we take the theoretical limiting values of 0 (good solvent) and 0.5 (θ-solvent). See also: Taylor, P. L.; Yu, Y.; Wang, X. Y. *J. Chem. Phys.* **1996**, *105*, 1237.
(23) Barrat, J.-L.; Joanny, J.-F.; Pincus, P. *J. Phys II* **1992**, *2*, 1531.
(24) Skouri, R.; Schosseler, F.; Munch, J. P.; Candau, S. J. *Macromolecules* **1995**, *28*, 197.
(25) Yamakawa, H. *Modern theory of polymer solutions*; Harper and Row: New York, 1971.

MA980355R